

Losses from long-living photoelectrons in terahertz-generating continuous-wave photomixers

E. A. Michael and M. Mikulics

Citation: [Appl. Phys. Lett.](#) **100**, 191112 (2012); doi: 10.1063/1.4711777

View online: <http://dx.doi.org/10.1063/1.4711777>

View Table of Contents: <http://apl.aip.org/resource/1/APPLAB/v100/i19>

Published by the [American Institute of Physics](#).

Additional information on Appl. Phys. Lett.

Journal Homepage: <http://apl.aip.org/>

Journal Information: http://apl.aip.org/about/about_the_journal

Top downloads: http://apl.aip.org/features/most_downloaded

Information for Authors: <http://apl.aip.org/authors>

ADVERTISEMENT

The advertisement banner features a background of orange and yellow diagonal stripes. At the top, the "AIP Applied Physics Letters" logo is displayed in white. Below the logo, on the left, is a white envelope icon. To the right of the envelope, the text "Accepting Submissions in Biophysics and Bio-Inspired Systems" is written in black. Further right, a white button with the text "Submit Today" in orange is visible. On the far right, the "AIP Publishing" logo is shown in blue and white.

AIP | Applied Physics Letters

Accepting Submissions in
Biophysics and Bio-Inspired Systems

Submit Today

AIP
Publishing

Losses from long-living photoelectrons in terahertz-generating continuous-wave photomixers

E. A. Michael¹ and M. Mikulics²

¹Department of Electrical Engineering, Universidad de Chile, Santiago, Chile

²Peter Grünberg Institut (PGI-9), Forschungszentrum Jülich, D-52425 Jülich, Germany and JARA-Fundamentals of Future Information Technology, Germany

(Received 5 February 2012; accepted 17 April 2012; published online 9 May 2012)

The extraction of continuous-wave terahertz (THz) power from photonic mixers is known to be hampered by input power limitations, low conversion efficiencies, and saturation effects. Using vertically illuminated low-temperature-grown GaAs travelling-wave mixers with a coplanar stripline geometry, a mechanism of illumination-dependent reabsorption of the THz-power generated by the mixer was isolated. We find evidence that it is related to a substantial density of long-living photoelectrons (several nanoseconds). The proposed mechanism is expected to impact the performance of photonic terahertz mixers at high input powers, also of those based on transit-time-dominated semiconductor structures. © 2012 American Institute of Physics. [<http://dx.doi.org/10.1063/1.4711777>]

Due to the initially assumed quadratic dependence of the terahertz (THz)-generating continuous-wave (CW) photonic mixers' output power on the near-infrared (NIR) input power, $P_{\text{THz}} = \eta \cdot (P_{\text{NIR}})^2$, high input power must be used to reach useful output power in response to the low efficiencies η observed in photonic mixers at submillimeter and THz frequencies.¹ In addition to this quadratic dependence, output power saturation mechanisms related to input power have been reported.^{1–3}

In this letter, we propose another mechanism for output power saturation related to input power which we expect to dominate at high input powers. The limiting pump power density for CW low-temperature (LT)-grown GaAs based mixers is about 1 mW/ μm^2 .¹ This results in power levels less than 100 mW for small-area (lumped-element) THz-photomixers, in which the optimum mixer area is determined by a tradeoff between desired speed (RC-constant) and pump power. Up to these typical power levels in small-area mixers, a slight deviation of the THz-output power has been reported,¹ $P_{\text{THz}} \propto (P_{\text{NIR}})^{2-\Delta}$, with $\Delta \approx 0.2\ldots 0.3$, explained by thermal effects.

In vertically illuminated travelling-wave (TW) photonic mixers, the mixer area limitation due to the RC-constant can be bypassed by an *in-situ* adjustment of the velocity-match between THz-wave and optical interference fringes.^{4–6} Using this technique, we applied 400 mW to our mixers, limited by our optical amplifier, typically illuminating an interdigitated stripline area of $2\ \mu\text{m} \times 150\ \mu\text{m}$ (FWHM).^{5,7,8} These intensities were comparable with those of lumped-element mixers, but typically stronger saturation was observed, with two contributions: the sub-linear behavior of the DC photocurrent $I_{\text{ph}}(P_{\text{NIR}})$ with input power (responsivity), explained by thermal effects; and a saturation in addition to the square law dependence of the THz-power on the DC photocurrent, $P_{\text{THz}}(I_{\text{ph}})$. This second contribution varied significantly between mixers of different materials and layer structures. Here, we propose that this additional saturation can be related to a reabsorption of the generated THz-field along the stripline by a high concentration of relatively long-living

(several nanoseconds) photoelectrons. These could be generated (1) in the “slow” semi-insulating (SI) GaAs substrate, separated from the stripline by the “ultra-fast” photoconducting LT-GaAs layer; (2) by charge screening induced delay of recombination,^{1,3} or (3) by scattering into metastable states in the fast layer itself, e.g., into the L valley.⁹ Absorption along striplines from free electrons in semiconducting substrates has rarely been investigated experimentally, so far only due to doping.^{10,11} However, free-carrier absorption in bulk GaAs has been well characterized.¹²

The density of those long-living photoelectrons would be in any case proportional to the photocurrent I_{ph} generated through the ultra-fast photoconductive layer connected to the striplines, therefore we assume $P_{\text{THz}} \sim I_{\text{ph}}^2 \cdot \exp(-\tilde{A} \cdot I_{\text{ph}})$, where \tilde{A} is a fit constant describing the saturation. The losses we discuss here were discovered when comparing thin and thick samples LT-GaAs, having thicknesses of 0.5 μm and 1.5 μm , respectively (Fig. 1(c)). This reabsorption is expected to be stronger in thin samples, because more long-living photoelectrons are generated nearer to the stripline electrodes. In order to test this hypothesis, a spatial separation between the THz generation and its proposed reabsorption is required (pump-probe experiment). The geometry of the vertically illuminated traveling-wave mixer allowed this effect to be isolated.

By modifying the regular free-space illumination (Fig. 1(a)) of the traveling-wave mixers,^{5,6} the THz-generating spot (pump-spot) is shifted 100 μm away from the antenna while the spot length is reduced from $\sim 150\ \mu\text{m}$ to $\sim 80\ \mu\text{m}$ FWHM (Fig. 1(b)) (focus width 2 μm). The THz-wave generated in the pump-spot travels towards the antenna, is radiated, and then detected by an InSb-hot-electron-bolometer (response-time 1 μs). Half of the input NIR power is used to generate a probe-spot by redirecting it over a beam splitter towards a grating G2. This grating is used to remove any phase front matching and therefore interference in order to generate a static density of photoelectrons in the probe-spot. It was verified that no THz-power was generated in the probe-spot even at very low beat frequencies, and by

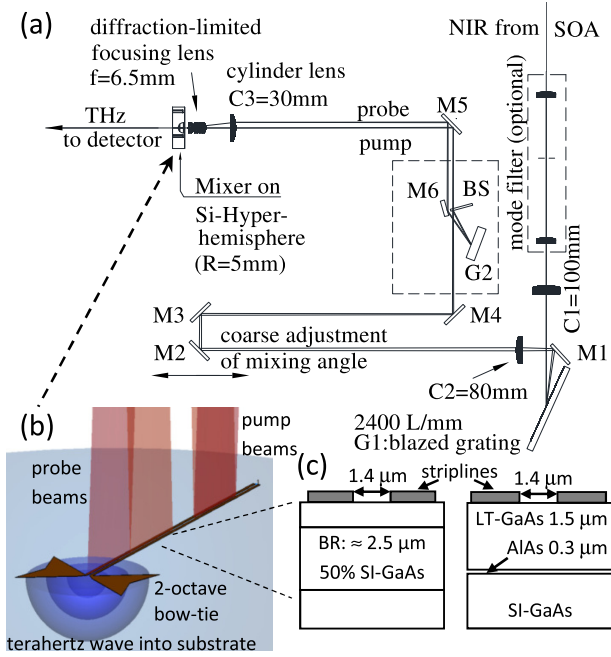


FIG. 1. (a) Optical setup to achieve angle self-tuning vertical illumination of the TW-photomixers, with added probe-beam path. The mode filter is not necessary using an interdigitated CPS (Ref. 5) or fiber illumination. (b) Pump and probe beams on the photomixer stripline. (c) Layer geometry of the thin and thick samples. The BR in the thin samples was erroneously fabricated using GaAs/AlAs instead of InGaAs/AlAs layers, so that NIR-absorption was also taking place there and a high reflectivity at 780 nm was not given. This was unfortunate with respect to obtaining good mixers, but gave rise to investigate the here proposed effect.

sweeping the probe-spot through the pump-spot, no interference could be observed in the THz-power generated. The probe beam is adjusted in parallel to the pump beam, a few mm away from it (see Fig. 1(a)), so that it is transferred into a focus position between pump-spot and antenna (Fig. 1(b)).

According to our hypothesis, the observed reduction of the THz-power caused by the probe beam can be written as $P_{\text{THz}}^{\text{probed}} = P_{\text{THz}}^0 \cdot \exp(-A \cdot I_{\text{ph}}^{\text{probe}})$, where P_{THz}^0 is the measured THz-power when no probe NIR-power is applied. The regular illumination of the TW-photomixers can be regarded as a pump-probe configuration in which the probe-beam is identical with the pump-beam. Therefore, \tilde{A} can be derived from A . While measuring $P_{\text{THz}}^{\text{probed}}$ and P_{THz}^0 , it was carefully verified that the bias voltage was constant. The illumination-related THz reabsorption constant, $\alpha_{\text{THz}}^{\text{illu}}$, in $P_{\text{THz}}^{\text{probed}} = P_{\text{THz}}^0 \cdot \exp(-\alpha_{\text{THz}}^{\text{illu}} \cdot L)$, depends on the coupled illumination density along the stripline like $\alpha_{\text{THz}}^{\text{illu}} = A' \cdot P_{\text{NIR}}^{\text{coupled}} / L$, so that the total THz absorption is independent of the length L of the illuminated probe section. The coupling efficiency of the probe beam to the stripline gap is much less compared to the pump beam because it passes off-axis through the last focusing lens system (see Fig. 1(a)) and therefore is not focused optimally to the aperture of the coplanar stripline (CPS). In any case, it is $P_{\text{NIR}}^{\text{coupled}} \propto I_{\text{ph}}^{\text{probe}}$ at constant bias voltage, and therefore $\alpha_{\text{THz}}^{\text{illu}} \propto n_{\text{e,SI-GaAs}} \propto n_{\text{e,LT-GaAs}} \propto I_{\text{ph}}^{\text{probe}}$.

In Fig. 2, the spatial optimization is explained and in Fig. 3 the measured values of the absorption constant as a function of frequency, $A(f)$, are plotted. Due to the antenna cut-off, values below 200 GHz could not be measured free-space, however, a data point at 40 GHz was accessible with a

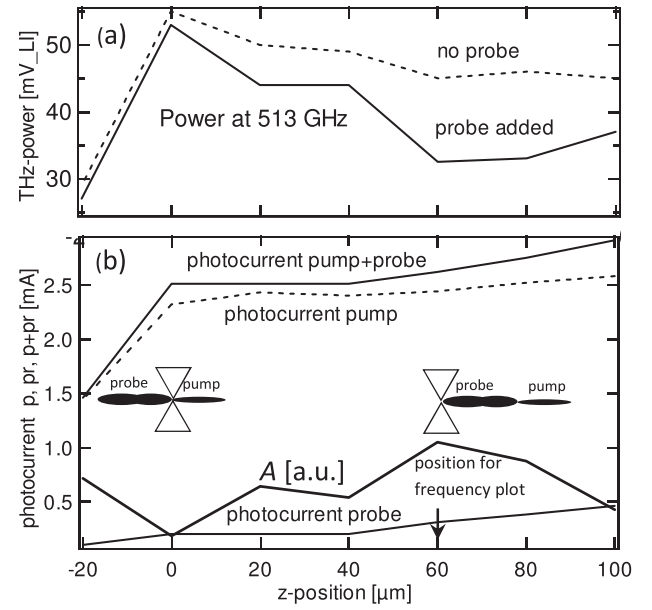


FIG. 2. (a) Measured THz-power with and without probe beam when stepping the photomixer block through the probe and pump beams, which are fixed in space, along the stripline (thin sample). (b) Photocurrents and THz reabsorption coefficient A . The two colors of the probe beam appear split by the grating G2.

network-analyzer through the illumination-related change of the S_{12} parameter between two SubMiniature A (SMA)-connectors wire-bonded to the antenna and the bias-pads, respectively.

The results could be confirmed when using a third diode laser for the probe beam, which had a frequency offset from those of the pump lasers by some THz.

The total losses along a CPS are given by $\alpha_{\text{THz}}(f) = \alpha_c \cdot \sqrt{f} + \alpha_r \cdot f^3 + \alpha_d(f)$, where α_c and α_r are the

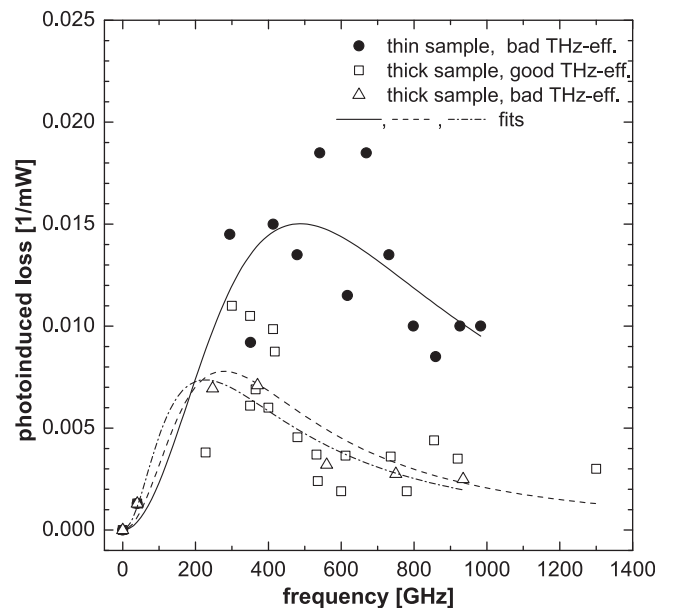


FIG. 3. Measured THz-losses $A := -1/P_{\text{NIR}}^{\text{probe}} \cdot \ln(P_{\text{THz}}^{\text{probe}}/P_{\text{THz}}^0)$ due to NIR-illumination with a probe beam as a function of THz-frequency for the samples with thick and thin LT-GaAs-layer, normalized by the estimated NIR probe power in the CPS gap. Good and bad THz efficiency refer to growth temperatures of 250 °C and 325 °C, respectively.

coefficients for stripline ohmic losses (within the skin depth) and radiation losses, respectively, and α_d is a function describing dielectric absorption.¹³

In order to find a form for the last term $\alpha_d(f)$, we first consider it for bulk material,¹² $\alpha(f) = 2k_0\kappa$, where $\kappa = \epsilon''/2n \approx \epsilon''/2n_\infty$ and n and κ are the real and imaginary part of the refraction index, respectively. ϵ'' is the imaginary part of the dielectric function $\epsilon = \epsilon' + i\epsilon'' = \epsilon_\infty + i\sigma/\epsilon_0\omega$. This results in the final form $\alpha(f) \approx \text{Re}\{\sigma(f)\}/(n_\infty c_0 \epsilon_0)$. Following this wave picture as a complementary one to transmission line theory,¹¹ an asymmetric THz-beam profile can be considered to propagate along the surface waveguide, and a part of it overlaps with regions of conductivity inside the material.

The conductivity σ is given by free electrons, described by the basic Drude model, $\sigma(\omega) = i\epsilon_0\omega_p^2/(\omega + i\cdot\Gamma)$. The plasma frequency $\omega_p^2 = n_e \cdot e^2/(m_e^*\epsilon_0)$ and the collisional damping rate of the electrons $\Gamma = \epsilon_0\omega_p^2/\sigma(0) = e/m_e^*\mu_e$ are both in the terahertz range.¹² Here, $m_e^* \approx 0.06 \cdot m_e$ is the effective Γ -valley electron mass, and $\mu_e \approx 8500 \text{ cm}^2 \text{ V}^{-1} \text{ s}^{-1}$ (Ref. 16) is the electron mobility in SI GaAs, so that $\Gamma \approx 3.4 \cdot 10^{12} \text{ Hz}$.

Pulse-propagation along a CPS was simulated in CST Microwave Studio, which uses frequency independent conductivities, for different depths and conductivities of the buried layer. From the S_{12} parameter absorption spectra were calculated, which showed indeed the expected increase with frequency, similar to the results of Ref. 11. Using sufficiently thick striplines and small CPS dimensions,⁵ the effects due to skin depth and radiation were small against substrate absorption, as compared against the absorption spectrum obtained with no conductivity.

Those absorption spectra could be fit by $1/[1 + (b/f)^2]$, a low-pass filter characteristic, which can be interpreted as a capacitive coupling from the CPS to the buried semi-conducting layer, where the energy is then dissipated, since the LT-GaAs layer has high resistivity even whilst illuminated. The fit-constant b was found to be dependent on the depth of that layer and its conductivity.

Multiplying the above fit with the frequency-dependence of $\text{Re}\{\sigma(\omega)\} = \epsilon_0\omega_p^2\Gamma/(\Gamma^2 + \omega^2)$, we obtain the function $A(f) = a/[(1 + (b/f)^2) \cdot (1 + (cf)^2)] \propto \alpha_d(f)$ to be fitted to the data of Fig. 3. The fits give values for Γ of 1–6 times its theoretical value.

In order to model the observed reabsorption, we used for the conductivities in the buried layer the values $\sigma(0) = e \cdot \mu_e \cdot n_e \approx 9000 \text{ S m}^{-1}$ underneath the thin sample LT-GaAs layer (incl. 50% dilution of GaAs in the Bragg reflector (BR)) and 2500 S m^{-1} underneath the thick LT-GaAs layer. These produced indeed THz-absorption values similar to the measured ones and were estimated by assuming $I_0 \approx 2 \cdot 10^7 \text{ W m}^{-2}$ ($P_{\text{probe}} = 60 \text{ mW}$ (effective), $w_{0z} \approx 150 \text{ }\mu\text{m}$, $w_{0x} \approx 4 \text{ }\mu\text{m}$) directly under the uncoated surface ($n = 3.3$), and $n_e(z) = R(z) \cdot \tau_e = I(z) \cdot \alpha_{\text{NIR}} \cdot \tau_e/h\nu$, with $\alpha_{\text{NIR}} = 1.5 \text{ }\mu\text{m}^{-1}$ at $\lambda = 780 \text{ nm}$ (Ref. 14) and $\tau_{e,\text{SI-GaAs}} = 5 \cdot 10^{-9} \text{ s}$.¹⁵

Consequently, in our case, the major effect could be clearly assigned to long-living photoelectrons situated in a buried layer and not in the ultrafast material,³ since no change with the bias-voltage was obvious, nor significant differences

with the quality of the ultrafast material could be found (see triangles (Δ) in Fig. 3). Moreover, no re-absorption could be found in 3 MeV ion-implanted samples.^{7,17}

To illustrate the magnitude of this effect, for example, we have computed the total THz power losses due to reabsorption from our measured A coefficient at 700 GHz for the thick LT-GaAs sample. The reduction in output power at 400 mW is 55% and the reduction at 1000 mW would be 86%. Indeed, in the 3 MeV ion-implanted material we investigated, the high defect density at large depth leads to a very short photoelectron lifetime and therefore negligible substrate free electron density at the respective depth. This could then explain why high-energy ion-implanted GaAs-mixers retain a square-law dependence of the output power up to higher input powers than LT-GaAs layer on SI-GaAs based mixers, resulting in an observed factor of three at 400 mW.⁷

In conclusion, this proposed loss due to reabsorption by long-living photoelectrons can result in large losses at high input powers, and due to the argued independence from scale length this would also be valid for lumped-element devices. The solution would be using non-NIR-absorbing substrates (e.g., transferring LT-GaAs to other substrates) or achieving ultra-short lifetimes also in the substrate (high-energy ion implantation).

Using such appropriate substrates and a refinement of the proposed CW pump-probe method (e.g., differential lock-in techniques and maybe a third far-off wavelength for the probe beam), it might be possible to disentangle in trap-time limited materials any reabsorption due to space charge effects³ (negative dependency on bias-voltage) or any reabsorption due to intrinsic generation of long living photoelectrons scattered into the side-valleys⁹ (positive dependency on bias voltage and dependency on the side-valley energies) from the here reported substrate effect.

The proposed mechanism is also expected to impact the performance of photonic submm-generating mixers based on transit-time dominated materials (e.g., p-i-n or UTC), since at the interesting illumination levels comparable electron concentrations ($>10^{23} \text{ m}^{-3}$) are present, and even nearer to the metallic striplines than reported here. As well, vertically illuminated TW-structures would be suited to characterize such mixer structures for this effect.¹⁸

E.A.M. acknowledges support by CONICYT Chile (Grants Fondecyt No. 1090306 and ALMA No. 31080020) and by Deutsche Forschungsgemeinschaft (Grant No. SFB 494, through J. Stutzki and R. Schieder of I. Physikalisches Institut, Universität zu Köln, Germany), and from I. Camara Mayorga and R. Güsten of Max Planck Institut für Radioastronomie, Bonn, Germany.

¹A. W. Jackson, Ph.D. dissertation, Materials Department, University of California, Santa Barbara, 1999.

²C.-K. Sun, I.-H. Tan, and J. E. Bowers, *IEEE Photon. Technol. Lett.* **10**, 135 (1998).

³G. C. Loata, T. Löffler, and H. G. Roskos, *Appl. Phys. Lett.* **90**, 052101 (2007).

⁴S. Matsuura, G. A. Blake, R. A. Wyss, J. C. Pearson, C. Kadow, A. W. Jackson, and A. C. Gossard, *Appl. Phys. Lett.* **74**, 2872 (1999).

⁵E. A. Michael, B. Vowinkel, R. Schieder, M. Mikulics, M. Marso, and P. Kordos, *Appl. Phys. Lett.* **86**, 111120 (2005).

⁶E. A. Michael, *Semicond. Sci. Technol.* **20**, 164 (2005).

- ⁷M. Mikulics, E. A. Michael, M. Marso, M. Lepsa, A. van der Hart, H. Lüth, A. Dewald, S. Stanček, M. Mozolik, and P. Kordoš, *Appl. Phys. Lett.* **89**, 071103 (2006).
- ⁸M. Mikulics, E. A. Michael, R. Schieder, J. Stutzki, R. Güsten, M. Marso, A. Förster, A. van der Hart, H. P. Bochem, P. Kordoš, and H. Lüth, *Appl. Phys. Lett.* **88**, 041118 (2006).
- ⁹A. Schwanhäuber, M. Betz, M. Eckardt, S. Trumm, L. Robledo, S. Malzer, A. Leitenstorfer, and G. H. Döhler, *Phys. Rev. B* **70**, 085211 (2004).
- ¹⁰H. R. Khazaei, O. Berolo, W. J. Wang, P. Maigne, M. Young, K. Ozard, M. Reeves, and F. M. Ghannouchi, *Proc. SPIE* **3491**, 90 (1998).
- ¹¹J.-H. Son, H.-H. Wang, J. F. Whitaker, and G. A. Mourou, *IEEE Trans. Microwave Theory Tech.* **41**, 1574 (1993).
- ¹²N. Katzenellenbogen and D. Grischkowsky, *Appl. Phys. Lett.* **61**, 840 (1992).
- ¹³S. Matsuura, G. A. Blake, R. A. Wyss, J. C. Pearson, C. Kadow, A. W. Jackson, and A. C. Gossard, in *Proceedings of the SPIE Conference on Terahertz and Gigahertz Photonics*, Denver, Colorado (SPIE, 1999), Vol. 3795, p. 484.
- ¹⁴H. C. Casey, D. D. Sell, and K. W. Wecht, *J. Appl. Phys.* **46**, 250 (1975).
- ¹⁵M. D. Sturge, *Phys. Rev.* **127**, 768 (1962).
- ¹⁶G. E. Stillman, C. M. Waife, and J. O. Dimmock, *J. Phys. Chem. Solids* **31**, 1199–1204 (1970).
- ¹⁷E. A. Michael, I. Camara Mayorga, R. Güsten, A. Dewald, and R. Schieder, *Appl. Phys. Lett.* **90**, 171109 (2007).
- ¹⁸C. Barrientos Z., V. Calle, M. Diaz, F. P. Mena, J. Vukusic, J. Stake, and E. A. Michael, *Proc. SPIE* **7741**, 77412L-5 (2010).